JTTEE5 22:756–763
DOI: 10.1007/s11666-013-9910-2
1059-9630/$19.00 © ASM International

Technical Note

Effect of Helmholtz Oscillation on Auto-shroud for APS Tungsten Carbide Coating

Younggil Jin, Sooseok Choi, Seung Jae Yang, Chong Rae Park, and Gon-Ho Kim

(Submitted September 29, 2012; in revised form February 6, 2013)

The atmospheric-pressure plasma spray (APS) of tungsten coating was performed using tungsten carbide (WC) powder by means of DC plasma torch equipped with a stepped anode nozzle as a potential method of W coating on graphite plasma-facing component of fusion reactors. This nozzle configuration allows Helmholtz oscillation mode dominating in APS arc fluctuation, and the variation of auto-shroud effect with Helmholtz oscillation characteristics can be investigated. Tungsten coating made from WC powder has lower porosity and higher tungsten purity than that made from pure tungsten powder. The porosity and chemical composition of coatings were investigated by mercury intrusion porosimetry and x-ray photoelectron spectroscopy, respectively. The purity of tungsten coating layer is increased with the increasing frequency of Helmholtz oscillation and the increasing arc current. The modulation of Helmholtz oscillation frequency and magnitude may enhance the decarburization of WC to deposit tungsten coating without W-C and W-O bond from WC powder.

Keywords atmospheric-pressure plasma spray (APS), auto-shroud effect, Helmholtz oscillation, in-flight oxidation, plasma facing component (PFC), tungsten carbide (WC)

1. Introduction

Nuclear fusion energy is one of the leading candidates for energy supply technologies and CO_2 mitigation technologies (Ref 1). In fusion power reactors, the plasma-facing component (PFC) requires high thermal durability under high flux over 10 MW/m^2 (Ref 2). Owing to high thermal conductivity, low tritium retention, and low erosion rate (Ref 3-5), high-Z materials such as tungsten are adopted for the PFC in the international thermonuclear experimental reactor (ITER) (Ref 6). Recently, tungsten-based PFC has been developed to reduce the economic burden which becomes enormous while using fully tungsten-armored first wall for an increased volume of reactor.

A solution for achieving tungsten-based PFC is performing tungsten coating by plasma spray method (Ref 7, 8). Although the W coating prepared using atmospheric-pressure plasma spray (APS) has advantages such as low cost and application with in situ repair, it showed relatively lower thermomechanical properties than a coating prepared using vacuum plasma spray (VPS) owing to the low oxygen content and porosity (Ref 9). The oxidation of W particles during APS is a critical issue that hinders the achievement of low porosity and high purity (Ref 10, 11). Thus, it is worthwhile to investigate how to improve the oxygen content and porosity in W coating process using APS.

A plasma jet with high specific enthalpy requires additional hydrogen gas (Ref 12, 13), which is accompanied by enhanced arc-fluctuation such as that in restrike mode and Helmholtz oscillation mode (Ref 14, 15). According to a previous report, a stepped nozzle suppresses the restrike mode because an arc root is located in enhanced turbulent region (Ref 16). Thus, arc voltage in a pure Helmholtz oscillation mode in the plasma torch with the stepped nozzle had a frequency of 4.5-5 kHz. The voltage characteristic was represented as a pseudo-sinusoidal waveform without the FFT peak of restrike at 2-5 kHz (Ref 14, 15, 17). The pure Helmholtz oscillation mode enhances the entrainment of ambient air during APS by developing turbulent eddies on the periphery of a plasma jet, corresponding to single- and high-frequency modes that intensify the piston motion of the plasma jet. In order to observe the auto-shroud effect enhanced by arc-fluctuation, the tungsten carbide (WC) is adopted because it is able to prevent the in-flight oxidation in atmosphere by decarburization of WC to W.

This study investigates the effect of Helmholtz oscillation on the in-flight oxidation of WC during APS. Experiments were carried out using a stepped nozzle torch which provides the Helmholtz oscillation mode dominated arc fluctuation, while frequency and magnitude of fluctuation varied with arc current (Ref 14). Experimental setup is described in section 2. The porosity and oxide content of the deposited layer are investigated with respect to the degree of air entrainment

Younggil Jin, Department of Energy System Engineering, Seoul National University, Seoul, Republic of Korea; **Sooseok Choi**, Department of Environmental Chemistry and Engineering, Tokyo Institute of Technology, Yokohama, Japan; **SeungJae Yang** and **ChongRae Park**, Carbon Nanomaterials Design Laboratory, Department of Materials Science and Engineering, Seoul National University, Seoul, Republic of Korea; and **Gon-Ho Kim**, Department of Energy System Engineering, Seoul National University, Seoul, Republic of Korea and Center for Advanced Research in Fusion Reactor Engineering, Seoul National University, Seoul, Republic of Korea. Contact e-mail: jinjun77@snu.ac.kr.

and the frequency modulation of the pure Helmholtz oscillation mode. It is discussed in section 3.

2. Experimental Setup

2.1 Plasma Spray System and Voltage Diagnostic

An APS system was prepared consisting of non-transferred DC plasma torch, DC power supply (Praxair, PS-100), torch transfer system, powder feeder (Sultzer Metco, Twin 10-C), and MFC gas supply for argon and hydrogen. The APS system was constructed with focus on promoting the high-frequency pure Helmholtz oscillation mode by means of a stepped nozzle. A non-transferred DC plasma torch equipped with the stepped nozzle prevents an arc-lengthening and a reattachment of arc root because an arc root is fixed by intensified turbulent stream line of an arc plasma jet existing in the torch interior region (Ref 16). It results in the restrike mode being stabilized in the stepped nozzle type of non-transferred DC plasma torch. A schematic of stepped nozzle and conventional cylindrical nozzle are shown in Fig. 1, which include tungsten cathode and copper anode. For clarity, based on Fig. 1, arc movement in the restrike mode is defined as a reattachment process along L_2 of cylindrical nozzle with oscillation while an arc behaviour in pure Helmholtz oscillation mode is characterized as oscillating hanging on periphery of L_3 exit without reattachment. L_2 and L_3 are defined as plasma oscillating chamber lengths in plasma region for cylindrical and stepped nozzle, respectively.

A frequency-diagnostic tool for an arc instability included a parallel resistance circuit composed of 50 and 5 kΩ for voltage division of 10:1, a voltage probe (Tektronix, 3Z80), and an oscilloscope (Tektronix, TDS 3032). An external resistance was chosen because of its sufficiently high enough value of resistance rather than for its load to detect arc voltage without current backflow to the oscilloscope. A sampling rate for FFT analysis was 5 Gs/s.

The spray distance from the torch exit to the substrate was 110 mm. Arc current had a wide range from 600 to 800 A for modulating a frequency of the pure Helmholtz oscillation mode based on the proportional relationship between the arc current (or enthalpy) and the characteristic oscillation frequency.

General governing equation for time transient pressure displacement as acoustic pressure wave is represented as follows (Ref 18):

$$m\frac{d^2\xi}{dt^2} + (R_r + R_\omega)\frac{d\xi}{dt} + s\xi = \mathrm{SP}e^{i\omega t} \qquad \text{(Eq 1)}$$

where P, and $\omega(2\pi f_\mathrm{H})$ are amplitude and frequency, respectively; ξ, S, and s are the pressure displacement, the neck of area of torch, and the effective stiffness, respectively. Therefore, the $\omega(2\pi f_\mathrm{H})$ and SP are representative factors of the Helmholtz oscillation frequency and the effective amplitude, respectively.

An acoustic resonance model was accepted for the Helmholtz oscillation frequency of f_H in nozzles of DC plasma torch (Ref 14). An equation can be defined as follows:

$$f_\mathrm{H} = \frac{1}{2\Pi}\sqrt{\left(Y_\mathrm{g}\frac{P_\mathrm{g}}{\rho_\mathrm{p}}\right)\left(\frac{S_3 I L_3}{S_1 L_1 + S_2 L_2}\right) \times \frac{1}{\sqrt{1 + \frac{\Pi d}{4L_3}}}} \qquad \text{(Eq 2)}$$

According to the equation, Helmholtz oscillation frequency of f_H has proportional relationship with isentropic

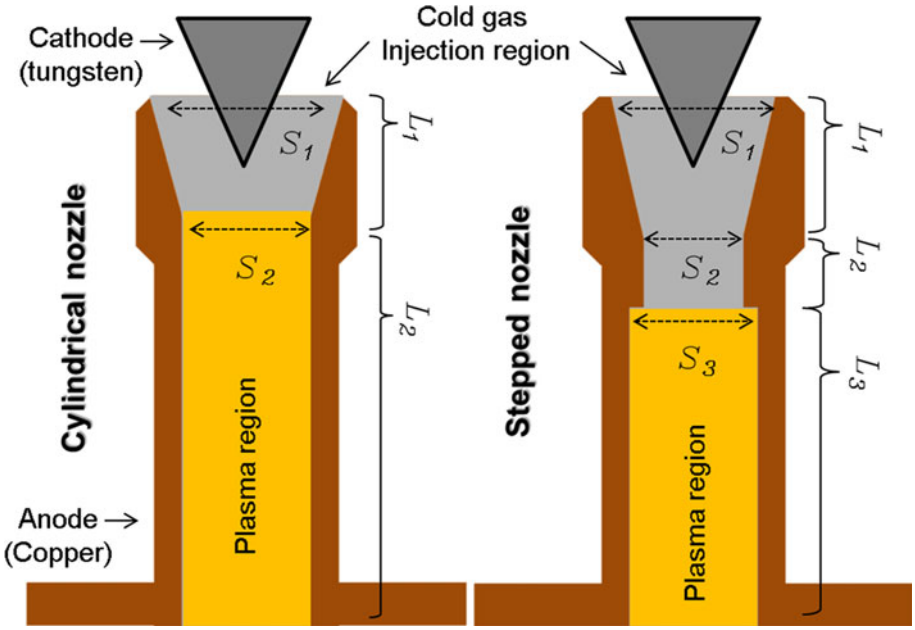

Fig. 1 Schematic of a conventional cylindrical nozzle (left) and a stepped anode nozzle (right) is represented. Nozzles are composed of tungsten cathode and copper anode. Cold gas injection port is near cathode region. S_1, S_2, and S_3 are the cross-sectional areas of nozzle while L_1, L_2, and L_3 are the length of nozzles for each diameter part

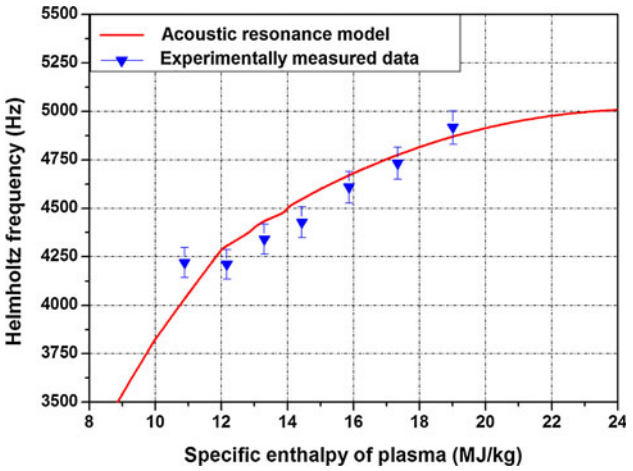

Fig. 2 The relationship between the Helmholtz frequency and specific enthalpy that is proportional to arc current. The *solid line* is obtained from the acoustic resonance model, while the *reverse triangles* represent the experimental results. The experimental result is well fitted to analytic model between 10 and 20 M/kg of plasma specific enthalpy range

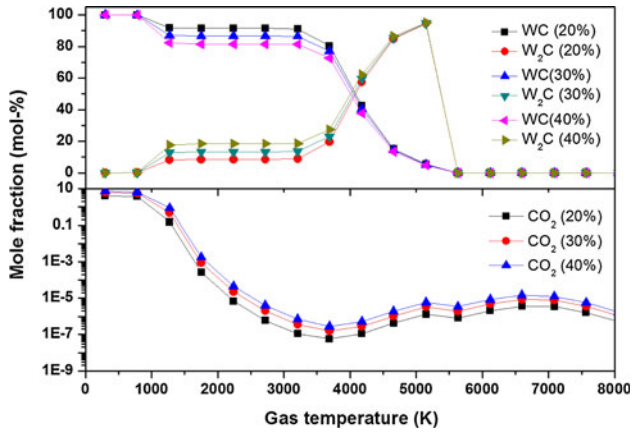

Fig. 3 The mole fractions of the chemical compounds that are calculated based on the thermodynamic database and minimum Gibbs free energy theorem for tungsten carbide. Expressed species are WC, W_2C, and CO_2. The mole fraction of WC decreased with proportional relationship with CO_2 concentration while W_2C increased proportional to CO_2 concentration for the whole temperature range of the gas. The variation of W_2C and CO_2 results from decarburization of WC as auto-shroud effect

exponent γ_g which is linearly increased with specific enthalpy in Ar/H_2 plasma jet of 10-20 MJ/kg. This trend is well illustrated in Fig. 2, which expresses the relationship between the specific enthalpy of plasma and the frequency of Helmholtz oscillation. Because the specific enthalpy is proportional to arc current, frequency modulation of Helmholtz oscillation is achievable with arc current control. In addition, the frequency could be changed with geometrical effects such as each cross-sectional areas of anode nozzles as S_1, S_2, and S_3 and each length as L_1, L_2, and L_3 as shown in the Fig. 1. P_g and ρ_p are the cold gas pressure and the plasma density, respectively; R_r and R_w are the acoustic radiation reactance and resistance, respectively. According to the definition of pressure amplification factor, Q is described by the following equation (Ref 18):

$$Q = \frac{\omega_0 m}{R_r + R_w} = \frac{\omega_0 m}{\frac{\rho_0 c k^2 S^2}{4\Pi} + R_w} \propto \frac{\text{const}}{\rho_0} \propto \text{SP} \qquad \text{(Eq 3)}$$

where Q represents the effective amplitude of Helmholtz oscillation, which is inversely proportional to gas density and input torch power. At the same pressure, density decreases with the increasing power (Ref 14). Thus, the torch input power increases both Helmholtz frequency and Helmholtz amplitude, which was implied in Eq 1.

2.2 Auto-shroud Effect of Tungsten Carbide

To evaluate the enhanced auto-shroud effect with the pure Helmholtz mode, tungsten carbide (Sultzer Metco, WOKA 3102 WC-12Co) powder that is 99.99 at.% of W-C compound with a diameter of 22 μm on average was used, and a tungsten (Sultzer Metco, 1061F) powder that was 99.99 at.% of tungsten with the same average diameter as WC powder was used for the reference coating to fabricate a tungsten-coated tile as PFC of high Z material.

Figure 3 is a mole fraction of WC which is dependent on oxygen concentration with variation along ambient gas temperature under the assumption of a local thermodynamic equilibrium (LTE) (Ref 19) state of thermal plasma jet. Based on LTE assumption, neutral gas temperature in the plasma jet could be considered as corresponding to plasma ion temperature, thus uniform temperature condition could be introduced except near the cold-gas boundary layer.

The mole fraction of each chemical state and compound was calculated using the thermodynamic database, which is based on the minimum Gibbs free energy and included the main reaction species such as WC(s), $WO_{2.72}$(s), W(s), W_2C(s), C(g), W(g), CO(g), WO_3(g), etc. For clarity, just WC(s), W_2C(s), and CO_2 (g) are depicted because the other compounds occupied very low concentrations. Thus, the chemical reaction chain mainly includes a decarburization of WC as an auto-shroud effect described by Eq 4 with variation of oxygen concentration. Thus, we can consider that main reactions of the plasma spraying of WC can be summarized as follows:

$$\text{(i) } 2WC(s) + 4O_2(g) \rightarrow 2W(s) + 2CO(g) + 3O_2(g) : \text{Decarburization(Auto - shroud)} \qquad \text{(Eq 4)}$$

$$\text{(ii) } 2W(s) + 3O_2(g) \rightarrow 2WO_3(S) : \text{Oxidation} \qquad \text{(Eq 5)}$$

$$\text{(iii) } W(s) \rightarrow W(l) : \text{Melting} \qquad \text{(Eq 6)}$$

$$\text{(iv) } W(l) \rightarrow W(g) : \text{Sublimation} \qquad \text{(Eq 7)}$$

The resultant chemical species of reaction (i) as auto-shroud effect are W and CO. According to the same, the reaction of auto-shroud effect precedes oxidation by protective CO atmosphere (Ref 20)and so auto-shroud effect

contributes to suppressing oxidation of tungsten, which accompanies the low reaction rate of sublimation. Based on Fig. 3, the rate of decarburization from WC to W_2C is proportional to dioxide concentration, implying a phenomenon induced by oxygen concentration, because the WC concentration is reduced with increment of oxygen concentration. Because the auto-shroud effect works in the whole range of temperature from 0 to 8000 K, the phenomenon is critical to decide the composition of WC powder during travelling the plasma jet.

A WC is a more sensitive material in the view of reaction range than that of tungsten in a temperature range for thermal plasma (1000-10,000 K) since decarburization was included in the total chemical reaction. In addition, the melting point of tungsten carbide (3143 K) was lower than that of tungsten (3695 K), while the oxidation temperature of tungsten carbide (~873 K) was higher than that of tungsten (~773 K) due to decarburization. Thus, the WC is more difficult to oxidize compared to tungsten due to the auto-shroud effect. Therefore, the degree of auto-shroud effect could be decided by entrained oxygen concentration from ambient air. In addition, the auto-shroud effect induces difference in the coating properties.

3. Results and Discussion

3.1 Arc Operating Mode of the DC Plasma Torch

An improvement of APS with WC powder was carried out in the view of modification of plasma jet interaction with ambient air, especially oxygen gas. Because WC is affected by auto-shroud effect, so it depends on CO gas generation from oxygen concentration as mentioned previously with Fig. 3, dependency of WC coating properties on the arc operating mode, which affects the degree of entrained ambient air during plasma spray, was investigated.

The arc operating mode was characterized from characteristic frequency spectrum for the plasma spray condition with an arc current at 600-800 A and gas flow rate of the argon/hydrogen was 45 and 5 (L/min). The characteristic frequency configuration of each mode was estimated from the FFT analysis.

Figure 4 shows the frequency spectrum of the pure Helmholtz mode at 4-5 kHz and the restrike mode at 2-3 kHz and 4-5 kHz, respectively. Obviously, a fluctuation of the arc voltage of the dc plasma torch during plasma spray distinguishes the pure Helmholtz mode from the restrike mode based on that the pure Helmholtz mode just has the Helmholtz oscillation frequency at 4-5 kHz and its harmonics. The Helmholtz oscillation dominant operation as pure Helmholtz mode is obtained from the stepped nozzle torch so hereafter it is named 'pure Helmholtz oscillation mode'.

The pure Helmholtz oscillation mode enhanced the entrainment of the ambient air into the plasma jet because the induced piston motion of plasma jet resulted in turbulent eddies on the periphery of the plasma jet. Consequently, an

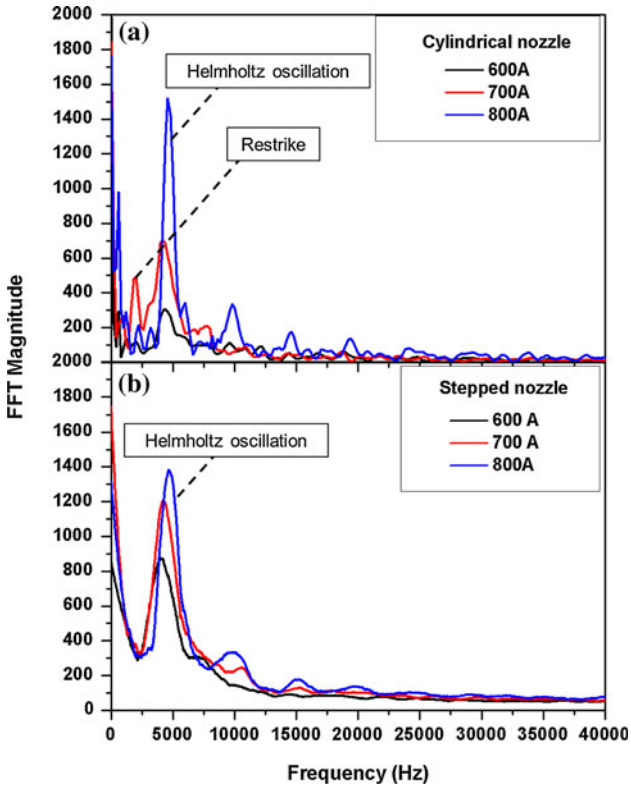

Fig. 4 The frequency spectrum of the restrike mode and pure Helmholtz mode was evaluated by FFT analysis for different spraying conditions of arc current 600, 700, and 800 A from the arc voltage signal during APS. Top plot is obtained from cylindrical nozzle torch and the bottom is from the stepped nozzle torch

enhancement of CO gas generation from oxygen concentration was proportional to the value of Helmholtz oscillation frequency, which increases with arc current increase.

The chemical composition of coating prepared by APS with WC powder is expected to depend on degree of auto-shroud effect rather than impact velocity of travelling particles. Thus, the dependency between chemical composition of the coating layer and frequency of Helmholtz oscillation was investigated in next section.

3.2 Chemical Composition of WC Coating Layer

WC coating layer was deposited by pure Helmholtz oscillation mode of DC plasma torch with frequency modulation. An assessment of the chemical uniformity was performed by x-ray photoelectron spectroscopy (Thermo VG, sigma probe) and XPS depth profile, by analyzing the atomic composition and chemical bonding. XPS has been extensively used to characterize the surface chemical features of various carbonaceous materials (Ref 21). The target was WC coating layer that was deposited with an arc current of 600, 700, and 800 A for APS in the pure Helmholtz oscillation mode.

Figure 5 shows the XPS spectra for the XPS depth profile from the surface to 120-nm depth and the curve-fitted bonding spectra for each spraying condition of arc

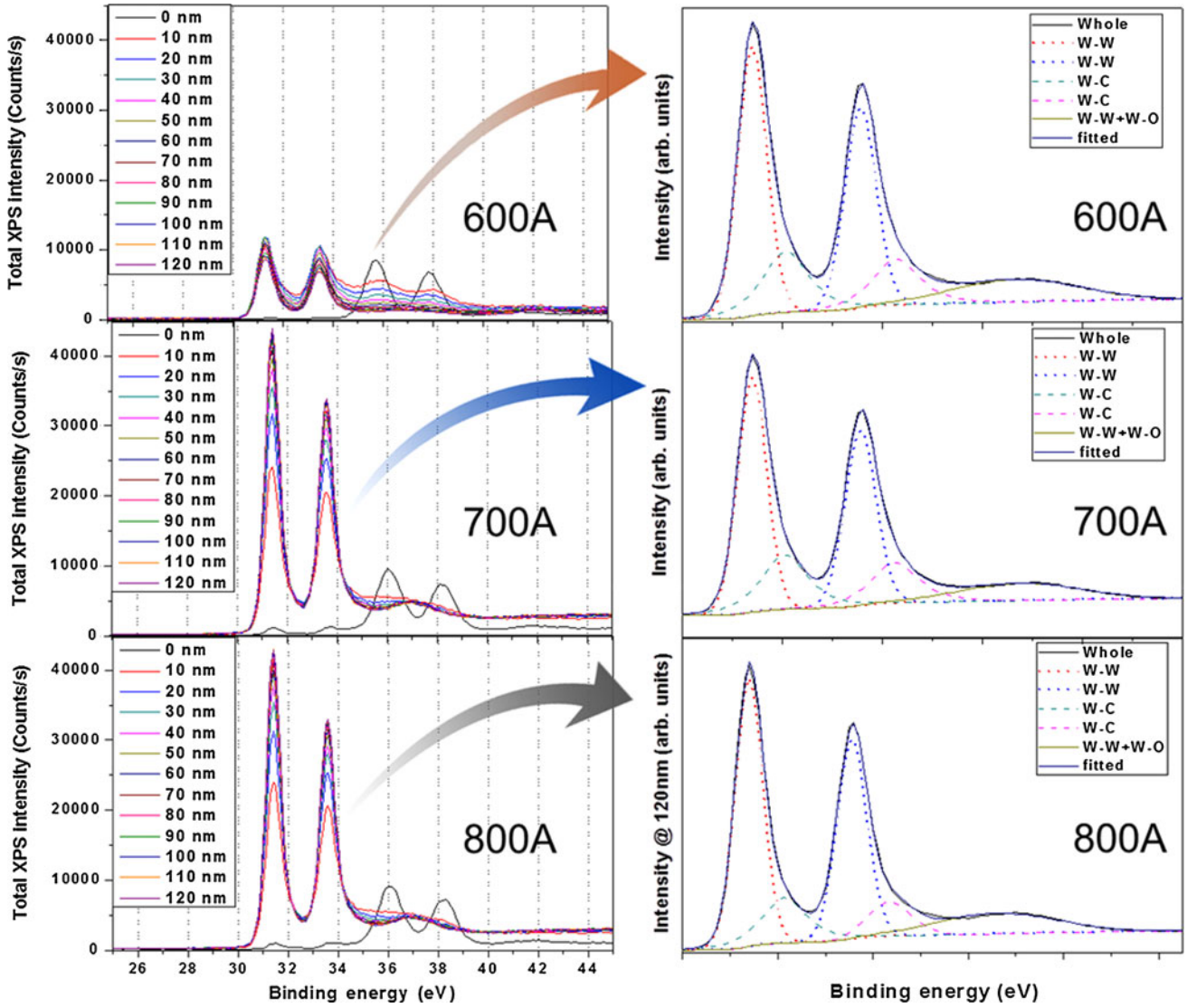

Fig. 5 XPS Spectra of the depth from surface to 120 nm (left) and surface (right) for the tungsten coating from tungsten carbide powder. Considered bonds are W-C (32.1, 34.3 eV), W-O (36.8 eV), and W-W (31.4, 33.6 eV)

current. 120 nm of depth is considered sufficient to detect the bulk properties of uniform coating layer. The curve-fitted spectra clearly show various bonding in the WC-coated layer. Nevertheless, even though the auto-shroud effect of the WC was attributed to decarburization, W-C (32.1, 34.3 eV) bonding still existed in the coated layer. It implies that a ratio between W-W bonding and W-C bonding can be used to evaluate the degree of auto-shroud effect during APS in the pure Helmholtz mode. The XPS spectra included W-O (36.8 eV) bonding as an evidence of oxidation of W. As a result of attribution of W-C and W-O bonding, the full width at half maximum (FWHM) values of the integrated curve-fits at 31.4 and 33.6 eV of bonding energy increased from 600 to 800 A, corresponding to greater amount of compound W-W.

A quantitative difference of the atomic composition between the tungsten coating and WC coating was evaluated with the XPS spectra, shown in Fig. 6. It appears that W4f7 indicates pure tungsten as a W-W bonding state. W4f7 means the most probable bond of W due to valance electron on orbital. In addition, the C1s means the carbon atom in the bulk coating layer and the O1s indicates the oxygen in the W-O state. The result demonstrates that the tungsten fraction (W4f7) increases from 70 to 95% with an arc current (600-800 A), while the carbon and oxygen fractions decrease depending on the arc current down to a minimum of 2%, implying that the auto-shroud effect of the WC is enhanced by the increases in the Helmholtz oscillation frequency from the pure Helmholtz mode.

The tungsten purity as chemical fraction of tungsten (W1f) shows proportional correlation with both

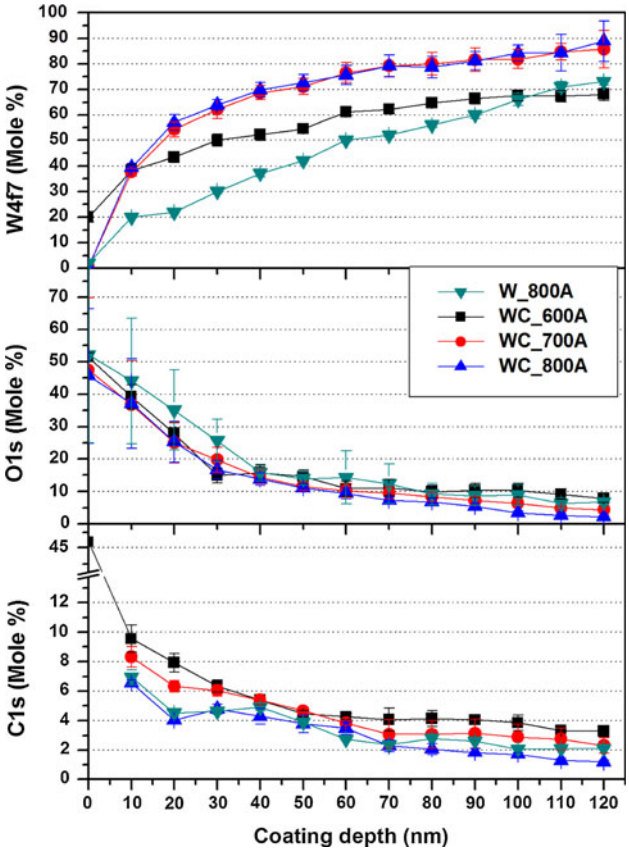

Fig. 6 Atomic composition of tungsten-coated layers with tungsten carbide powder was evaluated by XPS depth profile and curve-fit. The coating for 600 A (upper), 700 A (middle), and 800 A (bottom) are composed of W4f7, C1s, and O1s

Helmholtz magnitude and Helmholtz frequency as shown in FFT plot of Fig. 7, which represents proportional relationship between Helmholtz frequency and magnitude. As Helmholtz frequency is increased, XPS chemical composition of carbon (C1s) and oxygen (O1s) contents in the coating surface are decreased, implying the generation of CO gas as auto-shroud effect during in-flight time of WC. The plasma's specific enthalpy values of both conventional cylindrical torch and stepped nozzle were almost the same as shown in Fig. 8 so that the result shows a strict dependency of Helmholtz frequency in stepped nozzle torch, but not the specific enthalpy itself.

When considering this observation in conjunction with the result for the tungsten coating for 800 A case, for the comparison of the highest auto-shroud effect case of WC, the W4f7 approached 70% with the W4f7 (Oxide) in the bulk of the tungsten coating, whereas the W4f7 in the bulk of the WC was nearly 98%. In addition, the oxygen contents were about 5%, which was higher than the WC case (~2%). In fact, the pure Helmholtz mode enhanced the oxidation of the tungsten powder because there were no W-C bonds for decarburization. Therefore, the tungsten coating process with no WC but with tungsten has to be avoided when using plasma spray in the pure Helmholtz oscillation mode.

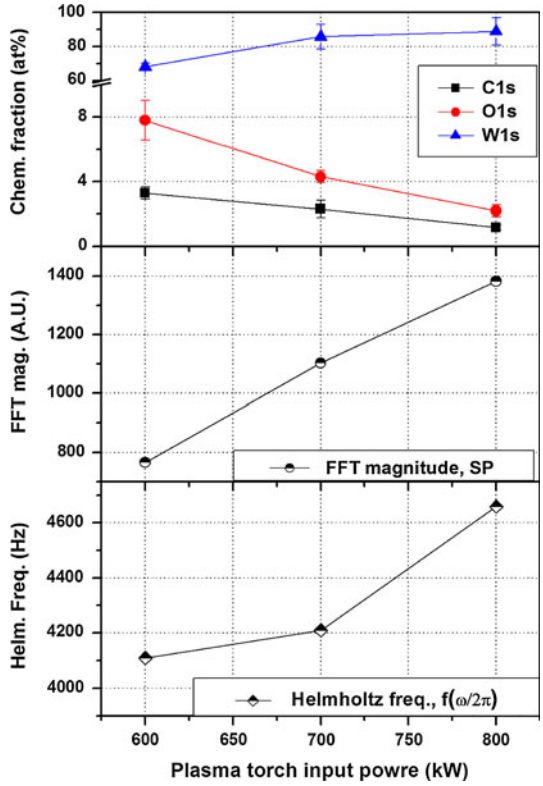

Fig. 7 Chemical fraction of tungsten coating layer that is from tungsten carbide powder with respect to plasma torch input power (top). Fast-Fourier transform (FFT) magnitude (middle) and frequency (bottom) of Helmholtz oscillation with respect to plasma torch input power

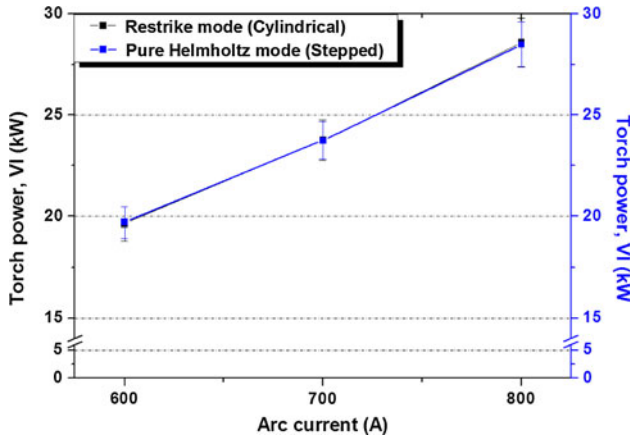

Fig. 8 Torch powers which are calculated by output average voltages and currents of conventional cylindrical nozzle torches and stepped nozzles. The variable is input arc current

3.3 Coating Microstructures and Porosity of WC Coating

In this study, a comparison of the macro and microstructures of the tungsten coating produced with tungsten powder and WC powder was performed. The field-enhanced-secondary electron spectroscopy (Carl Zeiss,

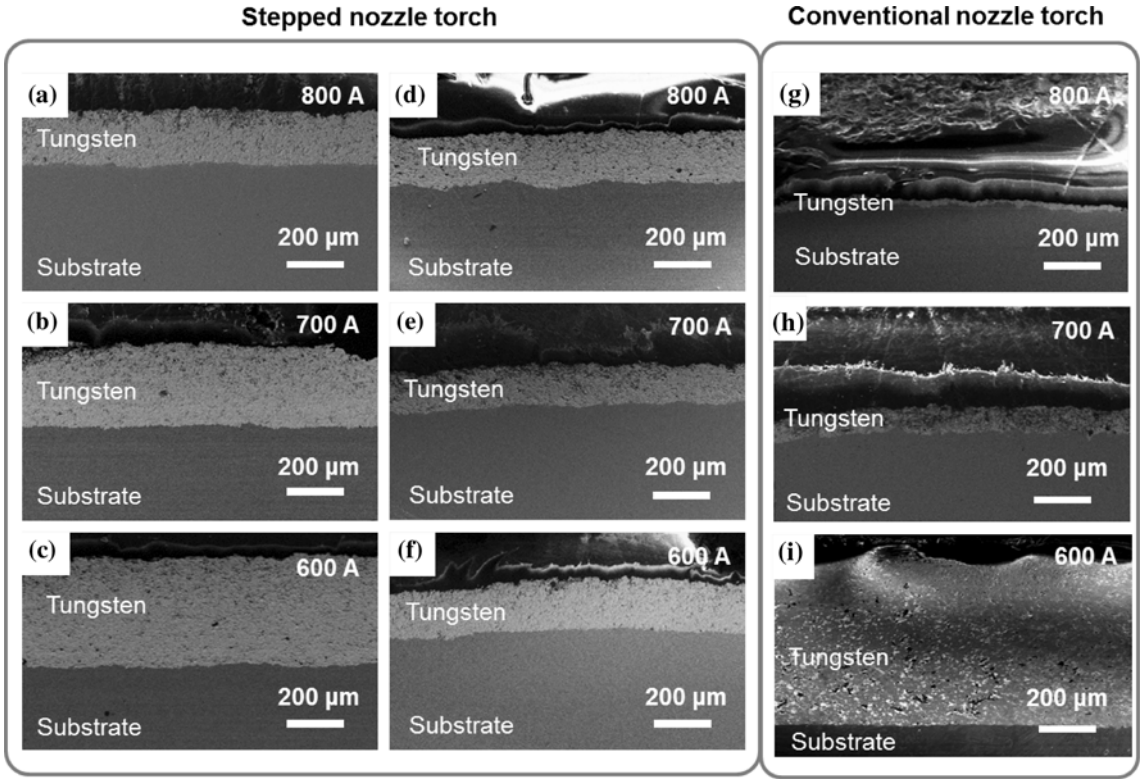

Fig. 9 The cross-sectional views of the tungsten coatings and tungsten carbide coatings captured by FE-SEM with various torch powers of 800, 700, and 600 A which are from top to bottom, respectively. (a)-(c) show the cross-sectionalviews of the tungsten coatings while (d)-(f) show the cross-sectional views of the tungsten carbide coatings. In addition, tungsten coatings which were deposited by conventional cylindrical nozzle torch are also shown. Coated part on the substrate is labelled by tungsten

SUPRA 55VP) image of a cross section of the coating on a stainless steel (SS 304S) substrate is shown in Fig. 9. The cross-sectional views of a tungsten coating made with tungsten powder are (a)-(c) and the tungsten coatings made with WC powder are (d)-(f). According to Fig. 9, it is clearly shown that the coated material is dense with an average coating thickness of about 200 μm for all cases (a)-(c) and (d)-(f).

Porosity of coating layers were measured by mercury intrusion porosimetry (Micromeritics, AutoPore IV 9500), being shown in Fig. 10. The error bar was calculated from the standard deviation of average value. The porosities of the coating layers were distinguishable between two materials in Fig. 10. The minimum porosity of the tungsten coating from WC powder is about 2%, which is lower than the porosity of the tungsten coating with tungsten powder (7%). In addition, an inverse proportion of the porosity on the torch input power is observed and a consistent trend of lower porosity of tungsten coatings from WC than tungsten powder is observed. Consequently, it represents that the tungsten carbide using stepped nozzle torch achieved the high-purity tungsten coating rather than tungsten powder.

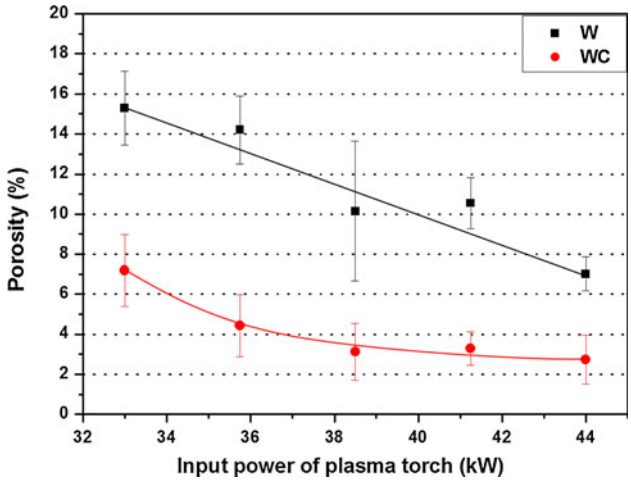

Fig. 10 The porosity of the coating layers fabricated using tungsten (W) and tungsten carbide (WC) powders with torch power ranging from 33 to 44 kW. The porosity was evaluated by automated porosimetry. Tungsten coating with tungsten carbide powder has lower porosities than tungsten coating with tungsten powder for the whole power range

4. Conclusions

An atmospheric plasma spray in the pure Helmholtz oscillation mode tends to facilitate deposits of high-purity and low oxidized tungsten coatings by enhancing the auto-shroud effect of the WC from WC powder because the auto-shroud effect of WC limits the in-flight oxidation of the carbon-detached tungsten powder by CO gas generation. In addition, the degree of the auto-shroud effect is proportional to the entrained oxygen concentration from the ambient air. The entrainment of the ambient air can be controlled in the pure Helmholtz mode operation as the intrinsic Helmholtz frequency and magnitude are controlled by torch input power. Therefore, the auto-shroud effect of WC could be enhanced by the plasma spray in the high-frequency pure Helmholtz mode using stepped nozzle with high input power.

Acknowledgments

This study was supported by Basic Science Research Program through the National Research Foundation of Korea funded by the Ministry of Education, Science and Technology (MEST) under the Project No. NRF-2012-0000578

References

1. K. Tokimatsu, Y. Asaoka, S. Konishi, J. Fujino, Y. Ogawa, K. Okano, S. Nishio, T. Yoshida, R. Hiwatari, and K. Yamaji, Studies of Breakeven Prices and Electricity Supply Potentials of Nuclear Fusion by a Long-term World Energy and Environment Model, *Nucl. Fusion*, 2002, **42**(11), p 1289-1298
2. P. Gavila, B. Riccardi, S. Constans, J.L. Jouvelot, I.B. Vastra, M. Missirlian, and M. Richou, High Heat Flux Testing of Mock-ups for a Full Tungsten ITER Divertor, *Fusion Eng. Des.*, 2011, **86**(9-11), p 1652-1655
3. A.A. Haasz, J.W. Davis, M. Poon, and R.G, Macaulay-Newcombe, Deuterium Retention in Tungsten for Fusion Use, *J. Nucl. Mater.*, 1998, **258**, p 889-895
4. R.A. Causey, Hydrogen Isotope Retention and Recycling in Fusion Reactor Plasma-Facing Components, *J. Nucl. Mater.*, 2002, **300**(2-3), p 91-117
5. H. Bolt, V. Barabash, W. Krauss, J. Linke, R. Neu, S. Suzuki, N. Yoshida, and A.U. Team, Materials for the Plasma-facing Components of Fusion Reactors, *J. Nucl. Mater.*, 2004, **329**, p 66-73
6. J. Marder, B. Rath, and S. Obenschain, International Thermonuclear Experimental Reactor, *Adv. Mater. Process.*, 2008, **166**(2), p 39-41
7. J.J. Huang, F. Wang, Y. Liu, S.S. Jiang, X.S. Wang, B. Qi, and L. Gao, Properties of Tungsten Coating Deposited onto Copper by High-Speed Atmospheric Plasma Spraying, *J. Nucl. Mater.*, 2011, **414**(1), p 8-11
8. Z.J. Zhou, S.Q. Guo, S.X. Song, W.Z. Yao, and C.C. Ge, The Development and Prospect of Fabrication of W Based Plasma Facing Component by Atmospheric Plasma Spraying, *Fusion Eng. Des.*, 2011, **86**(9-11), p 1625-1629
9. F.L. Chong, J.L. Chen, J.G. Li, D.Y. Hu, and X.B. Zheng, Heat Load Behaviors of Plasma Sprayed Tungsten Coatings on Copper Alloys with Different Compliant Layers, *J. Nucl. Mater.*, 2008, **375**(2), p 213-227
10. Y. Yahiro, M. Mitsuhara, K. Tokunakga, N. Yoshida, T. Hirai, K. Ezato, S. Suzuki, M. Akiba, and H. Nakashima, Characterization of Thick Plasma Spray Tungsten Coating on Ferritic/Martensitic Steel F82H for High Heat Flux Armor, *J. Nucl. Mater.*, 2009, **386-88**, p 784-788
11. D.Y. Hu, X.B. Zheng, Y.R. Nlu, H. Ji, F.L. Chong, and J.L. Chen, Effect of Oxidation Behavior on the Mechanical and Thermal Properties of Plasma Sprayed Tungsten Coatings, *J. Therm. Spray Technol.*, 2008, **17**(3), p 377-384
12. Y.I. Ishikawa, J. Kawakita, and S. Kuroda, Effect of Spray Condition and Heat Treatment on the Structure and Adhesive Wear Properties of WC Cermet Coatings, *Mater. Trans.*, 2003, **46**(7), p 1671-1676
13. E. Pfender, Thermal Plasma Technology: Where Do We Stand and Where are We Going?, *Plasma Chem. Plasma P*, 1999, **19**(1), p 1-31
14. J.F. Coudert, V. Rat, and D. Rigot, Influence of Helmholtz Oscillations on Arc Voltage Fluctuations in a DC Plasma Spraying Torch, *J. Phys. D Appl. Phys.*, 2007, **40**(23), p 7357-7366
15. Z. Duan and J. Heberlein, Arc Instabilities in a Plasma Spray Torch, *J. Therm. Spray Technol.*, 2002, **11**(1), p 44-51
16. S. Choi, T.H. Hwang, J.H. Seo, D.U. Kim, and S.H. Hong, Effects of Anode Nozzle Geometry on Ambient Air Entrainment into Thermal Plasma Jets Generated by Nontransferred Plasma Torch, *IEEE T Plasma Sci.*, 2004, **32**(2), p 473-478
17. H. Huang, W.X. Pan, Z.Y. Guo, and C.K. Wu, Instabilities in a Non-transferred Direct Current Plasma Torch Operated at Reduced Pressure, *J. Phys. D Appl. Phys.*, 2010, **43**(8)
18. L.E. Kinsler, A.R. Frey, A.B. Coppens, and J.V. Sanders, *Fundamentals of Acoustics*, 4th ed., Wiley, New York, 2000
19. A. Marotta, Determination of Axial Thermal Plasma Temperatures without Abel Inversion, *J. Phys. D Appl. Phys.*, 1994, **27**(2), p 268-272
20. V. Brožek, J. Matějíček, and K. Neufuss, Behavior of Tungsten Carbide in Water Stabilized Plasma, *Powder Metall. Progr.*, 2007, **7**(4), p 213-220
21. H. Kimura, Y. Nishikawa, T. Nakahata, M. Oyaidzu, Y. Oya, and K. Okuno, Chemical Behavior of Energetic Deuterium Implanted into Tungsten Carbide, *Fusion Eng. Des.*, 2006, **81**(1-7), p 295-299